Desalination and Water Treatment
www.deswater.com

doi: 10.5004/dwt.2017.21479

97 (2017) 251–261
November

Graft copolymerization of methyl acrylate onto date palm fiber and its application in the removal of chromium(III) from water

Abdalla Mohmoud Abulkibash[a,*], Nadir Mohammed Osman[a], Faraj Ahmad Abuilaiwi[b,*]

[a]*Department of Chemistry, King Fahd University of Petroleum and Minerals, Dhahran 32211, Saudi Arabia, email: abdallam@kfupm.edu.sa (A.M. Abulkibash)*
[b]*Department of Chemistry, University of Hafr Al Batin, Hafr Al Batin 31991, Saudi Arabia*

Received 21 March 2017; Accepted 22 September 2017

ABSTRACT

Toxic metals released from untreated industrial effluents can reach the water bodies and affect the aquatic life. These metals can easily enter the food chain and cause health hazards. Ion exchangers have been applied to remove certain ions from the polluted water. A new ion-exchanger was prepared by graft copolymerization of methyl acrylate onto date palm wood fiber in an aqueous solution. Hydrogen peroxide was used as an initiator and ferrous ammonium sulfate as a catalyst. The effects of the amount of the initiator, the amount of the catalyst, the reaction time and the reaction temperature were investigated. A maximum percentage of grafting of 220% and a grafting efficiency of 47% were obtained at a temperature of 90°C, a period of time of 2 h and an amount of 0.15 mmol of the catalyst. The optimum volume of the monomer was 8 mL and the concentration of hydrogen peroxide was 0.03 M. The grafted copolymer was characterized by Fourier transform infrared spectroscopy where a band at 1,730 cm^{-1} provides strong evidence of the grafting process. The surface morphology of the copolymer was studied using the scanning electron microscopy. The ion-exchanger was prepared by reacting the grafted copolymer with hydroxylamine hydrochloride. This ion-exchanger was applied for the removal of chromium from water.

Keywords: Graft copolymers; Date palm, Fibers; Methyl acrylate; Chromium; Ion-exchanger

1. Introduction

Several types of trees such as rubber, coconut and palm can provide valuable raw materials that have important applications. The date palm wood fiber (DPWF) is used in the construction of huts, aqueducts, bridges and its residues can be burnt for fuel [1]. The date palm has three major chemical components which are cellulose, lignin and hemicellulose as well as other minor constituents such as protein and oil [2,3]. Most of the wood fibers are hydrophobic and a wide range of chemical modifications have been developed to improve paint, stain and related coating or adhesives. These modifications generally provide physical interactions with the wood substrate but do not provide permanent modification for the wood surface. Chemical treatment through initiation of covalent bonds with the hydroxyl groups in external surface or in the walls of the cell may give excellent modification [4].

Grafting is considered as a powerful method that provides essential modification in the whole properties of the natural polymers. In addition, it also helps in retaining the desired specifications of the fiber [5].

Graft copolymerization is a technique commonly used to modify the chemical and physical properties of a polymer which will in turn lead to high strength, high modulus, toughness and low density. The resulting material will have a friendly impact on the environment. This approach has directed the attention to focus on the lignocellulosic biomass of eternal and annual plants as raw materials for the production of various advanced polymeric compounds [6].

Cellulose has many properties like renewability, biodegradability and can be modified to produce many useful products.

---

* Corresponding author.

1944-3994/1944-3986

Various plants can produce cellulose in their cells either as hair or as a structural polymer [7]. Therefore, wood is considered as the main source of cellulose where it exists as a texture combining with lignin. Cellulose can be modified by combining it with polar and ionizable groups. As a result, new polymeric materials have been synthesized and applied in industries like petroleum, papermaking, textiles and in the protection of environment [8]. Potassium persulfate has been used to initiate the graft copolymerization of methyl methacrylate onto cellulosic biofiber [9]. Recently, cellulose- and chitosan-based membranes have been introduced for water purification [10].

Some of the vinyl monomers have been applied in the graft copolymerization of cellulose. The resulting sorbents were so efficient to the extent that they have been used in water treatment processes [11,12]. In another study, the coconut husk was grafted with acetonitrile and used to remove mercury(II) from both aqueous solutions and wastewater of the chloro alkali industries [13]. The leaves of banana have been modified by introducing functional groups like phosphosulfonate, sulfate and phosphate and used to remove heavy metals ions [14]. New chelating materials have been prepared from sugarcane bagasse and used in the adsorption of metal ions from aqueous solutions [15,16]. Methylene blue (MB), cadmium(II) and copper(II) have been removed using a cheap solid adsorbent prepared from date pits [17]. Another low coast adsorbent has been prepared by physical modification of the wood sawdust which contains the texture of cellulose–lignin polymeric structure. This adsorbent has been used for the removal of copper(II) and iron(III) under variable conditions [18]. In addition, rice bran hemicelluloses and different chemically modified orange peel cellulose biosorbents possess the ability to adsorb some heavy metal ions effectively from aqueous solutions [19]. The potentiality of different agricultural waste wood in the removal of copper(II) has been studied [20]. Inorganic pollutants like cadmium, lead, chromium(III) and others are legally restricted to very low limits in aqueous effluents [21].

Chromium which exists in aqueous media as Cr(III) and Cr(VI) is considered as one of the most toxic heavy metals. Therefore, the World Health Organization and the United State Environmental Protection Agency have set a concentration of 0.05 mg/L for Cr(VI) and 0.1 mg/L for Cr(III) as the maximum allowable limits in drinking water [22].

Chromium is used in a wide spectrum of industries like metal production, paint, leather tanning, printing, textile agricultural and wood impregnation. These activities are responsible of discharging chromium into air, soil and water [23]. Wastewater released through these industries can contain 0.5–270 mg/L of Cr [23]. To a lesser extent chromium is also released to the environment from natural and anthropogenic sources [24].

Cr(III) potentiates the action of insulin in peripheral tissue and is essential for animals and human beings [25]. Food and Drug Administration has recommended a reference daily intake of 120 μg/d of chromium (US Department of Health and Human Services, 1995). On the other hand, Cr(VI) is a mutagen and is classified as a human carcinogen [21,25]. International Agency for Research on Cancer has classified chromium(VI) in Group 1 (carcinogenic to humans) and metallic chromium and chromium(III) in Group 3 (not classifiable as to their carcinogenicity to humans) [26]. Moreover, in studies with hamsters and mice, parenteral administration of chromium(III) or chromium(VI) during gestation did result in embryotoxicity or fetotoxicity and teratogenicity [27]. These effects appear to be associated with maternal toxicity, but definitive conclusions cannot be reached [28]. As a result, the US Environmental Protection Agency has set the maximum contamination level (MCL) for total Cr to 0.1 mg/L [24]. To a more stricter extent the WHO set the MCL of total Cr to 0.05 mg/L [21].

Various physicochemical techniques have been studied for the treatment of chromium metal pollution, such as chemical precipitation, ion-exchange, electrochemical precipitation, reduction, adsorption, solvent extraction, membrane separation, concentration, evaporation, reverse osmosis and biosorption and emulsion per traction technology [29]. These adsorption techniques have advantages like the reusability, low cost and higher capacity.

Graft copolymerization onto date palm fibers has not been investigated yet. This work was undertaken to prepare a low cost ion-exchanger by grafting methyl acrylate (MA) onto the date palm fibers. In this work, MA was used as a comonomer and H_2O_2/ferrous ammonium sulfate as an initiator. The optimum conditions for grafting were investigated by changing the reaction time, the reaction temperature, the concentration of H_2O_2 and the amount of ferrous ammonium sulfate used. The resulting grafted palm wood fiber was characterized by Fourier transform infrared (FTIR), scanning electron microscopy (SEM), thermogravimetric analysis (TGA) and derivative thermogravimetric analysis techniques. A poly(hydroxamic acid) ion-exchange resin was produced when hydroxylamine hydrochloride was allowed to react with the grafted palm wood fiber. This resin was applied for the removal of chromium(III) from aqueous media.

2. Experimental

2.1. Materials

The date palm fiber which was obtained from local farms was first ground to less than 200 μm. This fiber was washed twice with hot distilled water, then with acetone, and dried in an oven at a temperature of 50°C. MA (Merck, Germany) of 99% purity was purified by passing it through a column packed with an activated alumina to remove the inhibitor. Analytical reagent grade of hydrogen peroxide was purchased from Rirdel-de-Haen (Germany). Ammonium ferrous sulfate of an analytical grade was obtained from British Drug Houses and used as received. Other chemicals used were of analytical grade.

2.2. Graft copolymerization of date wood fiber

Graft copolymerization was carried out in a two-necked round bottom flask having a nitrogen gas inlet. The flask containing 100 mL of distilled water was placed in an oil bath of controlled temperature and equipped with a magnetic stirrer. An amount of 1.0 g of the fiber was added to the flask with constant stirring for a period of time of 5–10 min. A quantity of 0.1 g of ferrous ammonium sulfate was added under nitrogen atmosphere while the temperature of the solution was kept at 60°C for a period of 15 min. A quantity of 7.8×10^{-2} mol of the activated MA was added to the reaction mixture followed by a volume of 0.3 mL of 35% hydrogen peroxide with constant stirring. The temperature of the reaction mixture was maintained at 60°C for a period of 1 h. The reaction was stopped, the flask was cooled and the product was filtered. The final product was washed for several times with distilled water, dried in an oven at a temperature of 60°C and left for overnight and weighed. The dry product was washed with acetone in the Soxhlets apparatus for a period of 48 h. The final product was dried for overnight in an oven at a temperature of 60°C, then cooled and weighed.

2.2.1. Removal of homopolymer and determination of graft level

The crude product was purified with acetone using a Soxhlets extractor for 24 h to remove the polymethacrylate homopolymer. The pure grafted copolymers were then dried at 60°C to a constant weight. The percentage of grafting (P_g) was determined by the following formula:

$$P_g = \frac{w_2 - w_1}{w_1} \times 100 \tag{1}$$

where w_1 is the weight of the original DPWFs in grams, w_2 is the weight of the grafted product after copolymerization and extraction [30].

2.2.2. FTIR spectroscopy

Infrared (IR) spectra of the DPWF, grafted DPWF and the poly(hydroxamic acid) ion-exchange resin samples were recorded on an FTIR spectrometer (PerkinElmer 1725, Norwalk, CT) using a KBr disk pellet.

2.2.3. Scanning electron microscopy

The SEM photographs of the fiber surfaces of grafted polymethyl acrylate (PMA) onto DPWF and ungrafted DPWF were taken using a scanning electron microscope TESCAN model MIRA 3 LMU.

2.2.4. Thermogravimetric analysis

Thermogravimetric experiments were carried out using a Shimadzu TGA-50H Thermogravimetric Analyzer. The analysis was carried out under air atmosphere from ambient temperature to 700°C at a heating rate of 10°C/min.

2.3. Preparation of a chelating resin containing hydroxamic acid groups

A solution of hydroxylamine hydrochloride ($NH_2OH•HCl$) was prepared by dissolving an amount of 20 g of hydroxylamine hydrochloride in a volume of 300 mL of a solution of a volume ratio of 4:1 (methanol/water). The hydrochloride content of $NH_2OH•HCl$ was neutralized by the addition of NaOH solution and the precipitated NaCl was removed by filtration. The grafted product was placed in a two-necked flask equipped with a condenser, placed in a thermostat water bath and mixed with the hydroxylamine hydrochloride solution. The mixture was stirred and allowed to react for a period of 180 min at a temperature of 70°C. After completion of the reaction, the resin was filtered and washed several times with the methanolic solution. The resin was neutralized with a solution of 0.1 M HCl, then filtered, washed several times with the methanolic solution and dried to constant weight in an oven at a temperature of 60°C.

3. Results and discussion

The DPWF was treated with the initiator H_2O_2 and the cocatalyst ferrous ammonium sulfate solution. To this mixture, MA was added to form free radical sites. The copolymerization process starts by forming covalent bonds between the monomer and the fiber radicals where chain reactions propagate. In addition, a homopolymer of MA can occur due to the presence of the initiator in the reaction. Fig. 1 describes the mechanism of the grafting process [4].

3.1. Parameter optimization

3.1.1. Effect of temperature

The temperature of the grafting reaction was studied in the range of 30°C–120°C. It was found that the percentage yield of grafting has increased gradually up to 90°C where the maximum percentage yield of grafting was achieved. Increasing the temperature will affect the swellability of DPWF onto the substrate which can also increase the percentage yield of grafting. Such observation has been noted in the grafting of methyl methacrylate and oil palm empty fruit bunch [30] and MA onto the jute fiber [31]. In addition, increasing the temperature will increase the rate of diffusion of the monomer into the fiber matrix where grafting can be initiated by complexed monomer [32]. The temperature will also increase the rate of formation of the active primary radicals which will in turn increases the number of grafting sites. Above the temperature of 90°C the drop in the percentage yield of grafting is attributed to the decomposition of hydrogen peroxide which will furnish many radicals that enhance the formation of homopolymers as can be seen from Fig. 2.

3.1.2. Effect of the concentration of initiator

The percentage of grafting was found to increase with the concentration of the initiator up to a certain level then it starts to decrease as shown in Fig. 3. The increase in the concentration of the initiator will increase the number of free radicals in the system. This will in turn increase the number of the active sites in the backbone, hence, facilitate the grafting process. It is obvious from this figure that the maximum percentage of grafting has the value of 152. This value occurs at an initiator concentration of 0.03 M. Beyond this concentration, the percentage of grafting starts to decrease due to the formation of large numbers of cellulosic fiber radicals. These radicals may react with each other and terminate the reaction before the addition of the monomer. Moreover, homopolymerization is also possible at higher concentrations of the initiator [33].

3.1.3. Effect of the amount of monomer

Increasing the volume of the monomer (MA) from a volume of 2–8 mL was found to increase the percentage of grafting. A volume of 8 mL of the monomer was found to give a maximum percentage of grafting of 189% as shown in Fig. 4. More volumes of the monomer will initiate the homopolymerization process [33], as a result, the percentage of grafting will decrease.

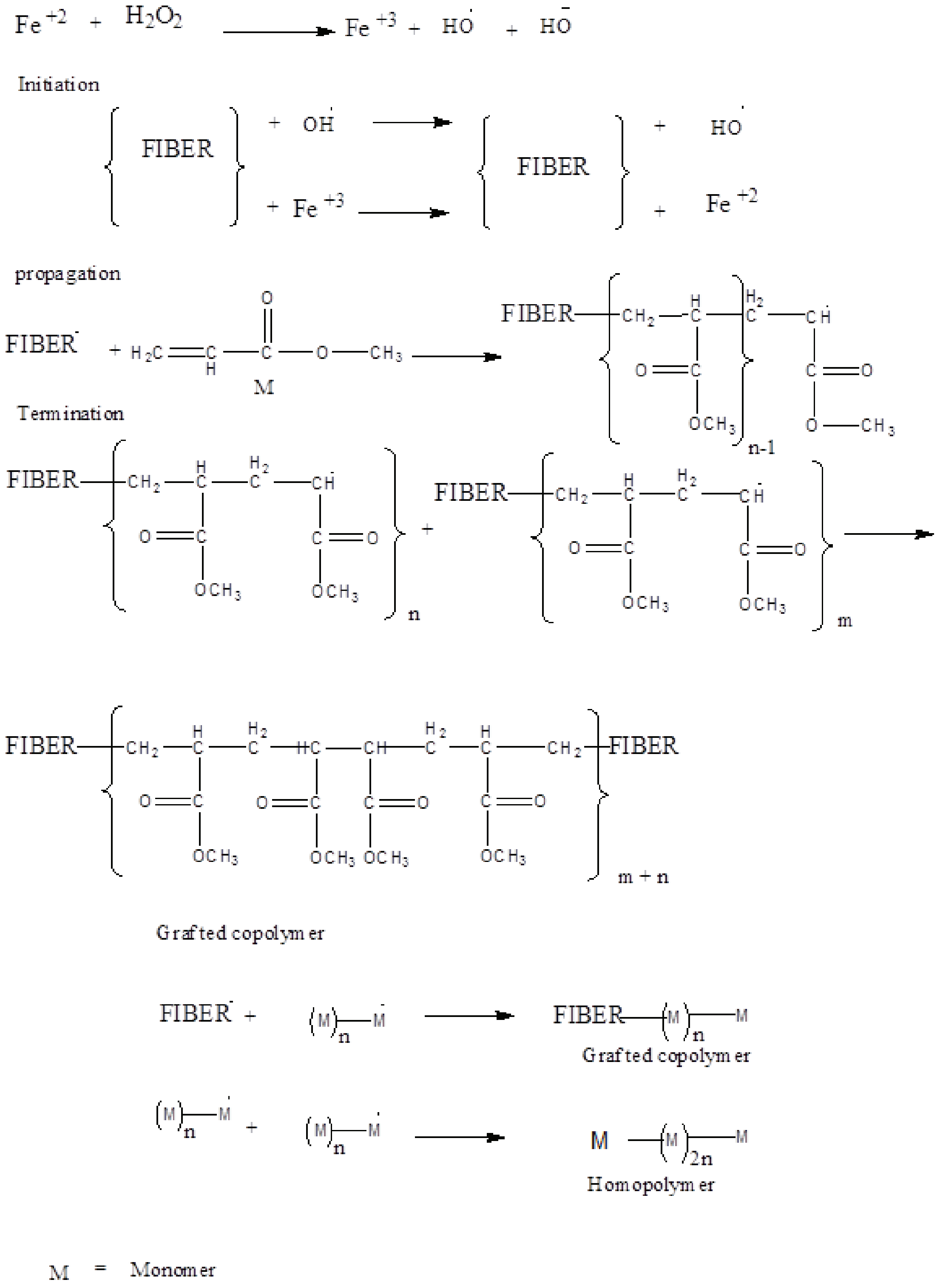

Fig. 1. Mechanism of graft copolymerization of MA onto DPWF.

3.1.4. Effect of reaction period

The grafting reaction was carried out during different periods of time that range from 30 to 150 min. Fig. 5 shows that a maximum percentage of grafting of 152% was obtained after 120 min. However, further increase in the time of the reaction will result in decreasing the concentrations of the monomer, the initiator and the catalyst. In addition, the active sites in the backbone will be covered with the polymer, hence, homopolymerization will be initiated [31,33] which will lead to a decrease in the percentage of grafting.

3.1.5. Effect of the amount of catalyst

The addition of a small amount of the catalyst to the graft copolymerization reaction was found to increase the percentage of grafting as shown in Fig. 6. A percentage of grafting of 206 has resulted when an amount of 0.15 mmol of ammonium ferrous sulfate [$(NH_4)_2SO_4.FeSO_4.6H_2O$] was used. This amount of catalyst is sufficient to decompose the hydrogen peroxide to generate the required amount of radicals. Further increase in the amount of the catalyst will lead to the formation of large numbers of free radicals that will interact and terminate the reaction [34].

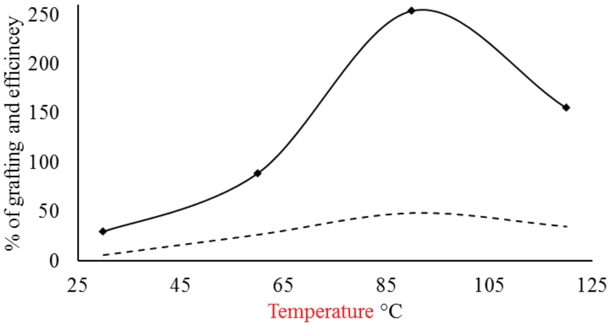

Fig. 2. Effect of reaction temperature on the grafting percentage (—) and grafting efficiency (---). Reaction time 120 min, MA 8.883 × 10^{-2} mol, H_2O_2 0.03 M, Fe^{2+} 0.01 mmol.

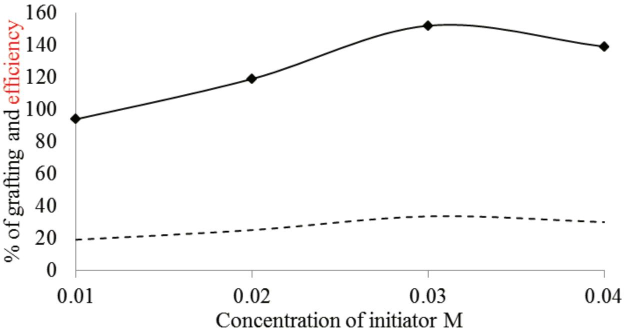

Fig. 3. Effect of the amount of initiator H_2O_2 on the grafting percentage (—) and grafting efficiency (---). Reaction time 120 min, MA 8.883 × 10^{-2} mol, temperature 90°C, Fe^{2+} 0.01 mmol.

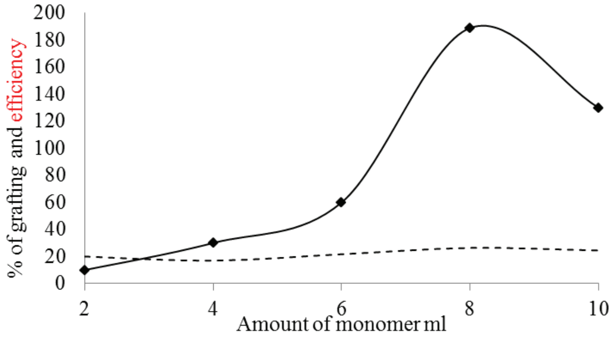

Fig. 4. Effect of the amount of monomer (MA) on the grafting percentage (—) and grafting efficiency (---). Reaction time 120 min, H_2O_2 0.03 M, temperature 90°C, Fe^{2+} 0.01 mmol.

3.1.6. Preparation of poly(hydroxamic acid) resin

The reaction between an ester and hydroxylamine in an alkaline medium is a general method to prepare hydroxamic acid. The same ratio of PMA-*grafted*-DPWF and hydroxylamine was used in alkaline media, the temperature of reaction was 70°C, the reaction was carried out during a period of 180 min in a methanolic solution (methanol/water ratio 80:20).

Domb et al. [35] suggested a mechanism for the reaction between polyacrylate ester with hydroxylamine to give poly(hydroxamic acid) which is shown in Fig. 7.

3.2. Characterization

3.2.1. Thermogravimetric analysis

TGA is a simple and accurate method for studying the decomposition pattern and the thermal stability of polymers. Figs. 8 and 9 show the thermogravimetric curves and the first derivative for date palm wood fiber (DPWF) and DPWF-g-PMA. Below 100°C, about 17% weight loss was observed in the PDWF due to the evaporation of moisture content [36]. Water formation from cellulose is known to occur at various temperatures in varying yields since there is a number of different water producing reactions during the degradation of cellulose. Cellulose in equilibrium with the atmosphere normally contains absorbed moisture due to its polar nature. Physical desorption of water occurs at a temperature range

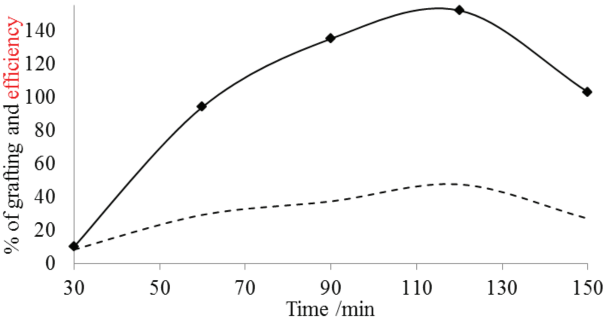

Fig. 5. Effect of reaction period on the grafting percentage (—) and grafting efficiency (---). MA 8.883 × 10^{-2} mol, H_2O_2 0.03 M, temperature 90°C, Fe^{2+} 0.01 mmol.

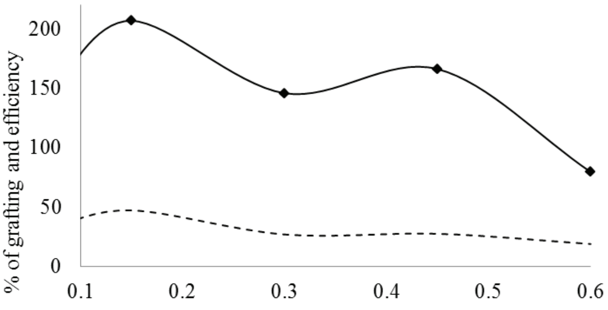

Fig. 6. Effect of the amount of the catalyst on the grafting percentage (—) and grafting efficiency (---). MA 8.883 × 10^{-2} mol, H_2O_2 0.03 M, temperature 90°C and a reaction time of 120 min.

of 25°C–150°C. However, when the cellulose is heated from a temperature of 150°C–320°C, water release was observed which could be attributed to the reaction of hydroxyl groups to form keto groups [37].

Graft copolymerization of vinyl monomers onto DPWF reduces its moisture content to about 5% in case of DPWF-g-PMA. In case of PDWF, the major degradation occurs between temperature of 220°C and 420°C leading to a weight loss of 70%, whereas in case of DPWF-g-PMA, the degradation occurs between temperature of 245°C and 500°C leading to a weight loss of 85%.

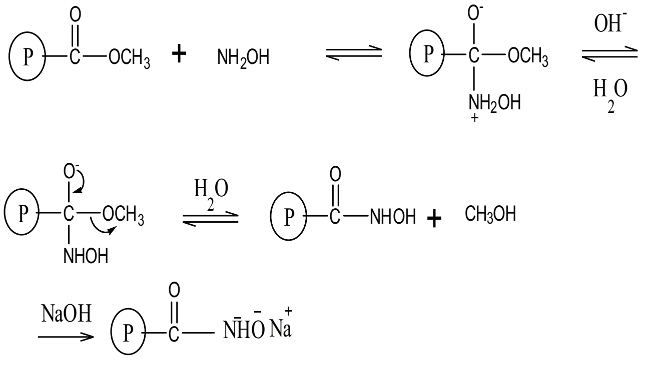

Fig. 7. Reaction mechanism of preparation of poly(hydroxamic acid).

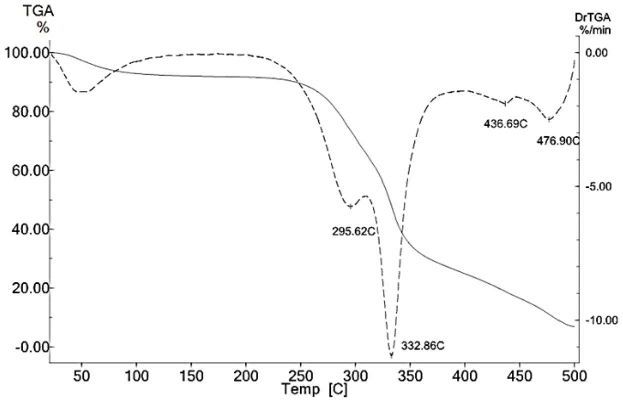

Fig. 8. Dynamic thermogravimetric (TG) and dynamic derivatives of the thermogravimetric (DTG) curves for palm date wood fiber at heating rate of 10°C.

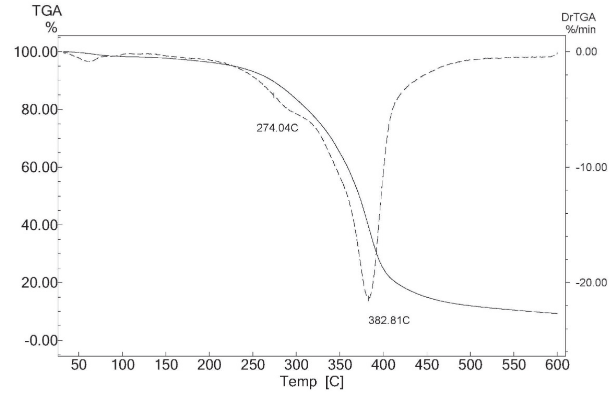

Fig. 9. Dynamic thermogravimetric (TG) and dynamic derivatives of the thermogravimetric (DTG) curves for palm date wood fiber grafted methyl acrylate at a heating rate of 10°C.

3.2.2. FTIR spectroscopy

FTIR spectroscopy was applied to characterize and verify the presence of the PMA on the DPWF and the hydroxamic acid group. Fig. 10 shows the FTIR spectra for DPWF, PMA-*grafted*-DPW fiber and the resin containing hydroxamic acid groups.

In the range of 3,100–3,500 cm^{-1} a broad absorption band characteristic to the hydroxyl group appears in all the spectra. This indicates the OH stretching vibrations of cellulose, absorbed water, hemicelluloses and lignin constituent of DPW.

A small peak around 1,740 cm^{-1} in the spectra of DPW shows the carbonyl stretching vibration of carboxyl groups in hemicelluloses and lignin in DPW. The increase in the intensity of the carbonyl peak (1,740 cm^{-1}) in the spectra of PMA-*grafted*-DPW fiber indicates that the presence of an ester group from MA. This is considered as a clear evidence of the grafting process. The band of 1,740 cm^{-1} characteristic to the C=O group has disappeared. A band at 1,646 cm^{-1} characteristic to the C=O of the hydroxamic acid has appeared in the spectrum of the resin.

Different absorption bands are shown in the two spectra. For instance, the band at 1,400–1,600 cm^{-1} indicates the presence of aromatic or benzene rings in lignin. Also, the band in the region of 1,000–1,300 cm^{-1} is indicative of the C–O stretching vibration of aliphatic primary and secondary alcohols in cellulose, hemicelluloses, lignin, and primary and secondary aromatic alcohols in lignin [4,30].

3.2.3. SEM microscopy

SEM was also applied to confirm the grafting of DPWF. Figs. 11 and 12 show the SEM images of micrograms of each of the DPWF and the PMA-*grafted*-DPWF, respectively. Fig. 9 shows clearly the pores on the surface of the DPW before grafting. However, after the grafting process those pores are fully covered as can be seen from Fig. 12 which represents the

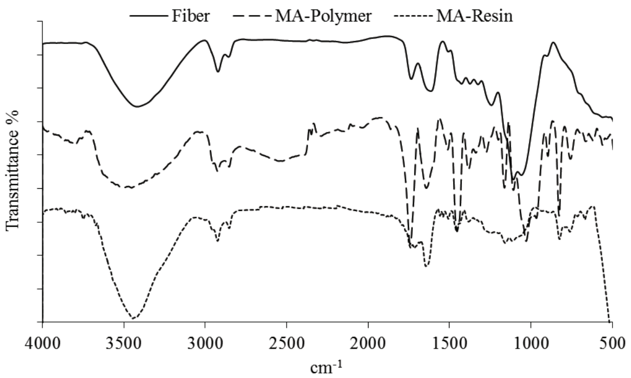

Fig. 10. FTIR DPWF (—), PMA-*g*-DPWF (---) and the resin containing hydroxamic acid groups (…).

PMA-*grafted*-DPWF. The surface is homogeneous because of the chemical bonds formed after the grafting process [30].

3.3. Adsorption studies

3.3.1. Effect of initial pH

The pH of the solution has a significant effect on the removal of heavy metals from aqueous solutions. The solubility of the adsorbates, the concentration of the counter ions and the degree of ionization of the adsorbate during the reaction are affected by the pH of the solution [38]. In this work, the effect of pH on the adsorption of Cr(III) was investigated using a fixed concentration of Cr(III) of 50 mg/L, 1.0 g of the resin, a reaction period of 1 h at a temperature of 25°C. The pH of the metal ion solutions was adjusted using the required volumes of 0.1 M acetic acid/sodium acetate buffer solution. Buffer solutions of a pH range of 1.0–6.0 were used to study the effect of the pH on the percentage removal of Cr(III). The pH range of 4–6 was found to be optimum where at pH 5 the percentage removal of Cr(III) was found to be 99.87%. In case of pH 4 and pH 6 the percentage removals were 39.75% and 98.52%, respectively, as can be seen from Fig. 13.

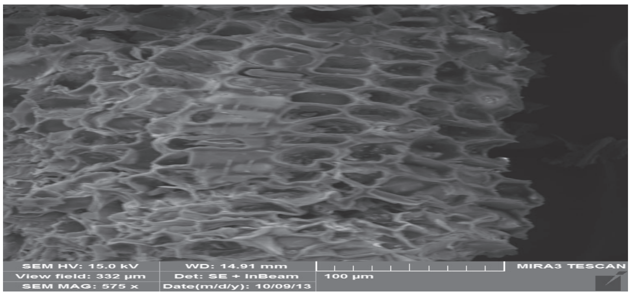

Fig. 11. Scanning electron micrographs of DPWF before grafting (575×).

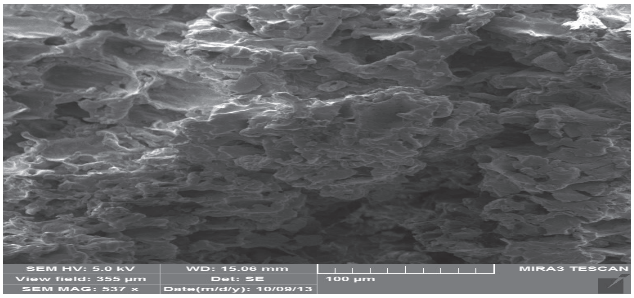

Fig. 12. Scanning electron micrographs of DPWF after grafting (575×).

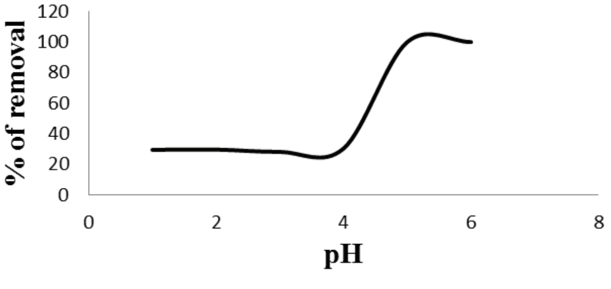

Fig. 13. Effect of pH on the adsorption of (Cr^{3+}) ions of a concentration of 50 mg/L, time 60 min and temperature 25°C.

3.3.2. Effect of contact time and the initial concentration of the Cr(III) on the removal

Fig. 14 shows the relationship between the adsorption of Cr(III) and the contact time using different initial concentrations of Cr(III) (30, 50 and 70 mg/L) at a pH of 5.5 and a temperature of 25°C. It is obvious from this figure that the amount of Cr(III) adsorbed increases with time and the adsorption is fast during the first period of 10 min. After the period of 10 min the adsorption slows down then becomes almost constant at the equilibrium point after a period of 40 min which is it gradually decreases to become constant at the equilibrium point. It is obvious from Fig. 12 which also shows that the amount of Cr(III) adsorbed, q_e (mg/g), increases with an increase of the initial concentration of the Cr(III).

3.3.3. Effect of adsorbent dosage

The adsorbent dosage is one of the important parameters that determine the adsorption capacity of an adsorbent for a given initial concentration. Fig. 15 shows the effect of increasing

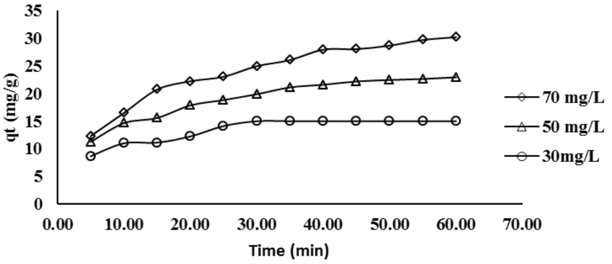

Fig. 14. Effect of the contact time on the adsorption of (Cr^{3+}) at different initial concentrations, at a solution pH 5.5 and a temperature of 25°C.

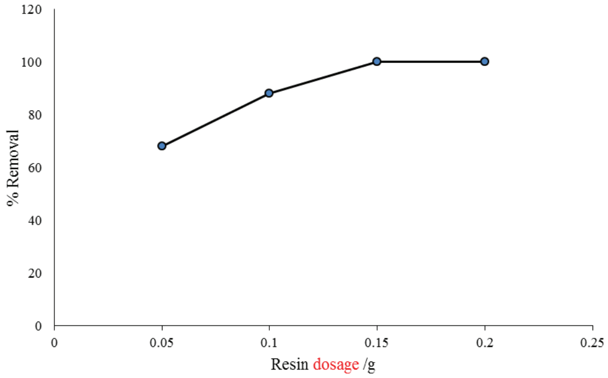

Fig. 15. Effect of adsorbent dosage on the adsorption of Cr(III) at pH 5.5, Cr(III) concentration 50 mg/L, time 60 min at a temperature of 25°C.

the adsorbent dose from 0.05 to 0.2 g/L of the resin on the adsorption of 50 mg/L of Cr(III) at 25°C. It was found that the percentage removal of Cr(III) has increased from 67.24% to 100.00% when the amount of the resin was increased from 0.05 to 0.2 g/L. This high percentage of Cr(III) removal can be attributed to the huge surface that has a great number of adsorption sites resulting from increasing the amount of the resin [39].

3.4. Adsorption kinetics

Adsorption kinetics explains the rate of the solute uptake at the solid–solution interface and provides important information about the reaction pathways and the mechanisms of the reactions. The kinetics of Cr(III) adsorption on the chelating resin was analyzed using pseudo-first-order, pseudo-second-order and intraparticle diffusion models. The agreement between the experimental data and the model predicted values was indicated by the correlation coefficients (R^2). A relatively high R^2 value indicates that the model successfully describes the kinetics of Cr(III) adsorption.

3.4.1. The pseudo-first-order equation

The pseudo-first-order equation, described in solid–liquid systems, is generally expressed as:

$$\log(q_e - q_t) = \log q_e - \frac{k_1 t}{2.303} \tag{2}$$

where q_t is the amount of Cr(III) adsorbed at time t (mg/g) and q_e is the amount adsorbed at equilibrium. k_1 is the rate constant of pseudo-first-order adsorption (per minute). Fig. 16 shows the resulting plots of the pseudo-first-order model for the adsorption of Cr(III) ions onto the chelating resin using three initial concentrations. The values of the rate constant k_1 and the adsorption density q_e which were obtained from the slopes and intercepts of the plots of $\log(q_e - q_t)$ vs. t are shown in Table 1. From this table, it is obvious that the values of the correlation coefficients (R^2) obtained are low. In addition, the resulting plots are of poor linearity. Furthermore, the apparent disagreement between the experimentally observed equilibrium adsorption (q_e, experimental) and the theoretically derived (q_e, calculated) using Eq. (3). As a result one can conclude that indicate that the adsorption mechanism of Cr(III) on the surface of chelating resin cannot be explained using the pseudo-first-order kinetic model.

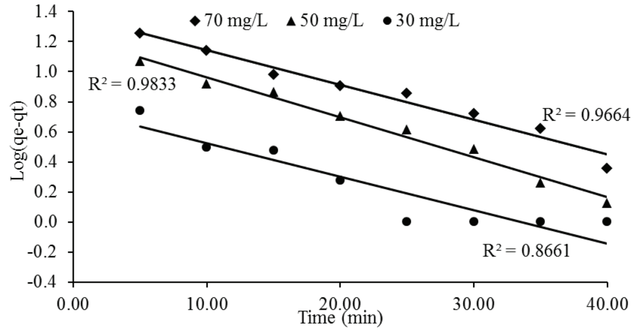

Fig. 16. Lagergren first-order plot for Cr(III) adsorption on the chelating resin for three initial concentrations at pH 5.5 and a temperature of 25°C.

3.4.2. The pseudo-second-order equation

The pseudo-second-order adsorption kinetic model was investigated using the equation:

$$\frac{\mathrm{d}q_t}{\mathrm{d}t} = k_2 (q_e - q_t)^2 \tag{3}$$

where q_e and q_t are the adsorption capacities at equilibrium and at time t (mg/g), respectively, k_2 is the rate constant of the pseudo-second-order adsorption (mg/g/min). For the boundary conditions $t = 0$ to $t = t$ and $q_t = 0$ to $q_t = q_t$, the integrated form of Eq. (3) will be:

$$\frac{1}{q_e - q_t} = \frac{1}{q_e} + k_2 t \tag{4}$$

which is the integrated rate law for a pseudo-second-order reaction. On rearranging Eq. (4), Eq. (5) which has a linear form is obtained:

$$\frac{t}{q_t} = \frac{1}{k_2 q_e^2} + \frac{t}{q_e} \tag{5}$$

The initial adsorption rate, h (mg/g/min) is given as:

$$h = k_2 q_e^2 \tag{6}$$

Eq. (5) can be written as:

$$\frac{t}{q_t} = \frac{1}{h} + \frac{t}{q_e} \tag{7}$$

From Eq. (5), the plots of t/q_t vs. t give a linear plot which is shown in Fig. 17. The values of q_e (calculated) and k_2 which are adsorption parameters were determined

Table 1
Kinetic constant parameters obtained for Cr(III) adsorption on chelating resin

Adsorbate	Pseudo-first–order						Pseudo-second-order			Intraparticle diffusion model		
	C_i (mg/L)	$q_{e,\mathrm{exp}}$ (mg/g)	K_1 (10^{-3}) (min^{-1})	$q_{e,\mathrm{cal}}$ (mg/g)	R^2	K_2 (10^{-2}) (g/mg min)	$q_{e,\mathrm{cal}}$ (mg/g)	h (g/min)	R^2	k_{id} (mg/g min)	C (mg/g)	R^2
Chromium(III)	70	30.24	53.2	1,451.4	0.966	0.22	36.23	2.86	0.997	2.834	9.0232	0.972
	50	22.96	61.02	670.2	0.983	0.33	20.96	1.44	0.973	1.615	4.8067	0.975
	30	14.12	51.4	53.1	0.866	2.06	15.94	5.23	0.999	0.667	10.486	0.756

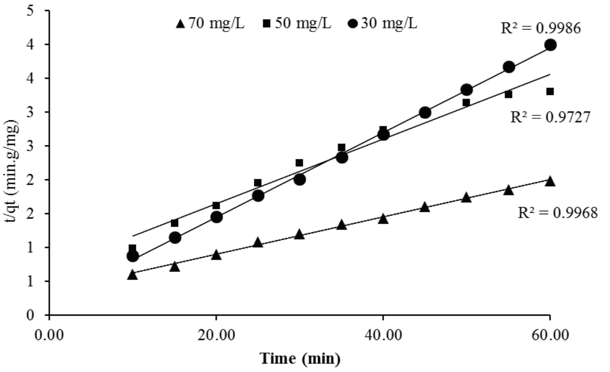

Fig. 17. Pseudo-second-order kinetic plot for Cr(III) adsorption on chelating resin for different initial feed concentration at pH 5.5 and temperature 25°C.

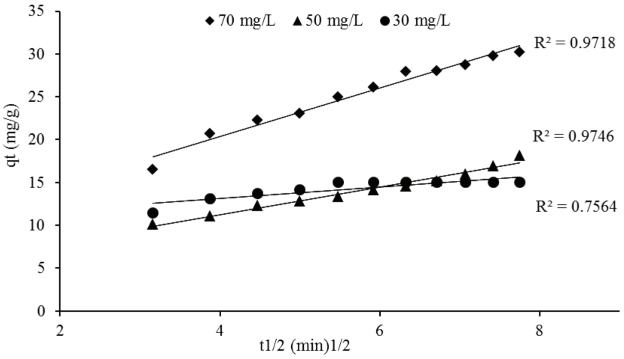

Fig. 18. Intraparticle diffusion kinetic plot for Cr(III) adsorption on chelating resin for different initial feed concentration at pH 5.5 and temperature 25°C.

from the slopes and intercepts of the plots, respectively (Table 1). The values of the correlation coefficients (R^2) obtained from the pseudo-second-order kinetic model are large. Moreover, the equilibrium adsorption capacity ($q_{e,\text{cal}}$) derived from Eq. (5) also agrees well with the experimentally observed data. These results indicate that the adsorption of Cr(III) on the chelating resin belongs to the second-order kinetic model, where the Cr(III) ions are adsorbed on the surface of the resin via chemical interaction such as ionic or covalent bonding [40].

3.4.3. The intraparticle diffusion model

The mechanism of adsorption of Cr(III) ions on the chelating resin was identified by testing the experimental data of adsorption process using the intraparticle diffusion model. Many consecutive steps may involve in the sorption of an adsorbate by a porous solid adsorbent, which are, first, the place where the adsorbate moves from the bulk solution to the external surface of the adsorbent which is called surface diffusion. Second, the movement of the molecules into the interior of the adsorbent particles and this is called intraparticle or pore diffusion. Third, the adsorption of Cr(III) ions on the interior sites of the resin. The intraparticle diffusion model is expressed as:

$$q_t = k_{\text{id}} t^{1/2} + C \quad (8)$$

where k_{id} is the intraparticle diffusion rate constant (mg/g/min$^{1/2}$), C is the intercept (mg/g) the plots of q_t vs. $t^{1/2}$ are shown in Fig. 18. It is clear that the lines of all the studied concentrations do not pass through the point of origin. This indicates that adsorption mechanism seems to be very complex.

3.5. Adsorption isotherm models

Various isotherm models were applied to determination of adsorption efficiency in the adsorption of heavy metals from aqueous solution, and the importance of the adsorption isotherms the description of the fraction of sorbate molecules that are split between liquid and solid phase at equilibrium. Langmuir and Freundlich adsorption isotherm models were studied for the adsorption of Cr(III) on the chelating resin.

3.5.1. The Langmuir isotherm model

The Langmuir model presumes that the adsorbent has a homogenous surface with a finite number of adsorption sites that accommodate the adsorbate species in a monolayer form [41]. The surface of the adsorbent will reach the saturation point when all the adsorption sites are filled by the adsorbate species and there is no chance for more adsorption to take place. The linear equation is expressed as:

$$\frac{C_e}{q_e} = \frac{1}{K_L q_m} + \frac{C_e}{q_m} \quad (9)$$

where q_e is the amount of Cr(III) ions adsorbed (mg/g) at equilibrium. C_e is the equilibrium concentration (mg/L) of Cr(III) in solution, q_m gives the maximum theoretical monolayer adsorption capacity (mg/g) and K_L is Langmuir equilibrium constant (L/mg) which is related to the affinity of adsorption sites.

From the plot of C_e/q_e vs. C_e, the values of q_m and K_L can be obtained from the slope and the intercept, respectively. The correlation coefficients (R^2) can also be obtained from Table 2. The linearity of the plot (Fig. 19) indicates that the Langmuir adsorption isotherm which assumes the formation of a monolayer on the surface of the adsorbent is applicable in this study. Moreover, the experimental data shows a high correlation with the Langmuir model. For this model, the separation factor (R_L) defined by Weber and Chakkravorti [42], is a characteristic dimensionless equilibrium parameter.

$$R_L = \frac{1}{1 + K_L C_0} \quad (10)$$

where K_L (L/mg) is the Langmuir constant and C_0 (mg/L) is the lowest initial concentration of Cr(III). From the average value of (R_L), Table 2, which is greater than zero and less than unity for each initial concentration. This indicates the favorable adsorption of Cr(III) on the chelating and the isotherm data fits well with this model.

3.5.2. The Freundlich isotherm model

The Freundlich model is used to study the adsorption on a heterogeneous surface. The mass of the chelating resin is

Table 2
Langmuir and Freundlich isotherm constants for Cr(III) adsorption on Chelating resin

Adsorbate	T (K)	Langmuir isotherm constants				Freundlich isotherm constants			
		q_m (mg/g)	K_L (L/mg)	R_L	R^2	$1/n$	n	K_F	R^2
Chromium(III)	298.16	42.74	5.32	0.004	0.999	0.06	15.43	49.74	0.9701

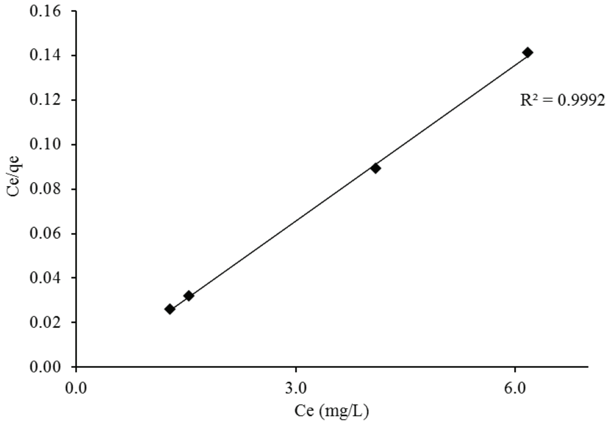

Fig. 19. Langmuir adsorption isotherms for Cr(III) adsorption on a chelating resin, pH 5.5 and a temperature of 25°C.

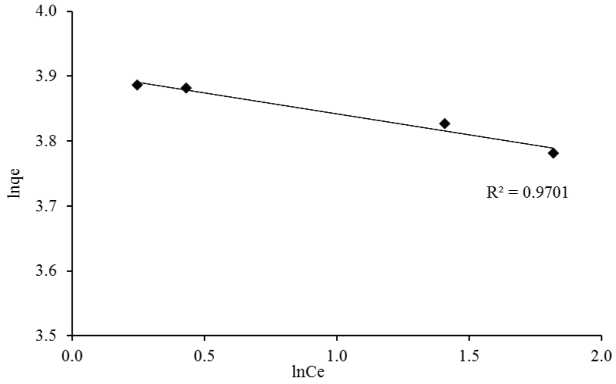

Fig. 20. Freundlich adsorption isotherms for Cr(III) adsorption on a chelating resin, pH 5.5 and temperature 25°C.

fixed and the various initial concentrations of Cr(III) were used to obtain the equilibrium data. The linear equation of Freundlich isotherm model is:

$$\ln q_e = \ln K_F + \frac{1}{n}\ln C_e \tag{11}$$

where K_F (mg/g) and $1/n$ (g/L) are Freundlich adsorption constants, indicating the adsorption capacity and adsorption intensity, respectively.

lnq_e against lnC_e was plotted and straight lines were obtained for the adsorption of Cr(III) on the chelating resin as can be seen from Fig. 20. The values of Freundlich adsorption constants K_F and n were calculated from the intercept and the slope of the same plot and listed in Table 2, the values of correlation coefficient (R^2) give an indication of a poor agreement between the experimental data and the Freundlich model. Also, the value of $n > 1$ represents a favorable adsorption condition, which means that Cr(III) ions are favorably adsorbed by the prepared chelating resin [43].

4. Conclusions

DPWF was grafted with MA monomer using hydrogen peroxide as an initiator and ammonium ferrous sulfate as a catalyst. Parameters that affect the grafting process include the amount of the catalyst, the concentration of the initiator, the volume of the monomer, the time and the temperature of the reaction were studied. The optimum conditions that give a highest percentage of grafting of 220% were found to be: 0.15 mmol of the catalyst, 0.03 M H_2O_2, 8 mL MA, a reaction time of 2 h and a temperature of 90°C. FTIR data and the SEM micrographs of the purified product confirmed the completion of grafting process. An ion-exchanger was prepared and used for the removal of chromium ion from water.

Acknowledgments

The authors would like to acknowledge the support provided by King Abdulaziz City for Science and Technology (KACST) through the Science and Technology Unit at King Fahd University of Petroleum and Minerals (KFUPM) for funding this work through project No. 11-WAT2170-04 as part of the National Science, Technology and Innovation Plan.

References

[1] K. Karimi, M.J. Taherzadeh, Critical review of analytical methods in pretreatment of lignocelluloses: composition, imaging, and crystallinity, Bioresour. Technol., 200 (2016) 1008–1018.
[2] D. Stylianos, K. Stefanidis, G. Kalogiannis, F.E. Iliopouloua, C.M. Michailof, A.P. Pilavachi, A. Angelos Lappas, A study of lignocellulosic biomass pyrolysis via the pyrolysis of cellulose, hemicellulose and lignin, J. Anal. Appl. Pyrolysis, 105 (2014) 143–150.
[3] T. Ahmad, M. Danish, M. Rafatullah, A. Ghazali, O. Sulaiman, R. Hashim, M.N.M. Ibrahim, The use of date palm as a potential adsorbent for wastewater treatment: a review, Environ. Sci. Pollut. Res., 19 (2012) 1464–1484.
[4] F.A. Abu-Ilaiwi, M.B Ahmad, N.A. Ibrahim, M.Z. Ab Rahman, K.Z.M. Dahlan, W.M.Z.W. Yunus, Optimized conditions for the grafting reaction of poly-(methyl acrylate) onto rubberwood fiber, Polym. Int., 53 (2004) 386–391.
[5] E. Princi, S. Vicini, N. Proietti, D. Capitani, Grafting polymerization on cellulose based textiles: a ^{13}C solid state NMR characterization, Eur. Polym. J., 41 (2005) 1196–1203.
[6] B. Focher, A. Marzetti, E. Marsano, G. Conio, A. Tealdi, A. Cosani, M. Terbojevich, Regenerated and graft copolymer fibers from steam-exploded wheat straw: characterization and properties, J. Appl. Polym. Sci., 67 (1998) 961–974.
[7] B. Imre, B. Pukánszky, From natural resources to functional polymeric biomaterials, Eur. Polym. J., 68 (2015) 481–487.
[8] Y. Tan, L. Zhang, Z. Li, Synthesis and characterization of new amphoteric graft copolymer of sodium carboxymethyl cellulose with acrylamide and dimethylaminoethyl methylacrylate, J. Appl. Polym. Sci., 69 (1998) 879–885.

[9] V.K. Thakur, A. Singha, M.K. Thakur, Graft copolymerization of methyl acrylate onto cellulosic biofiber: synthesis, characterization and applications, J. Polym. Environ., 20 (2011) 532–544.

[10] V.K. Thakur, S.I. Voicuuz, Recent advances in cellulose and chitosan based membranes for water purification, Carbohydr. Polym., 146 (2016) 148–165.

[11] N. Biçaka, D.C. Sherrington, B.F. Senkal, Graft copolymer of acrylamide onto cellulose as mercury selective sorbent, React. Funct. Polym., 41 (1999) 69–76.

[12] A. Kumar, K. Santhana, M. Barathi, S. Puvvada, N. Rajesh, Microwave assisted preparation of glycidyl methacrylate grafted cellulose adsorbent for the effective adsorption of mercury from a coal fly ash sample, J. Environ. Chem. Eng., 1 (2013) 1359–1367.

[13] P. Miretzky, A.F. Cirelli, Hg(II) removal from water by chitosan and chitosan derivatives: a review, J. Hazard. Mater., 167 (2009) 10–23.

[14] A.M.A. Nada, A.A. El-Gendy, S.H. Mohamed, Banana leaves as adsorbents for removal of metal ions from waste water, Carbohydr. Polym., 82 (2010) 1025–1030.

[15] E.M. Soliman, S.A. Ahmed, A.A. Fadl, Reactivity of sugar cane bagasse as a natural solid phase extractor for selective removal of Fe(III) and heavy-metal ions from natural water samples, Arabian J. Chem., 4 (2011) 63–70.

[16] O.K. Junior, L.V.A. Gurgel, R.P. de Freitas, L.F. Gil, Adsorption of Cu(II), Cd(II), and Pb(II) from aqueous single metal solutions by mercerized cellulose and mercerized sugarcane bagasse chemically modified with EDTA dianhydride (EDTAD), Carbohydr. Polym., 77 (2009) 643–650.

[17] M.A. Al-Ghouti, J. Li, Y. Salamh, N. Al-Laqtah, G. Walker, M. N.M. Ahmad, Adsorption mechanisms of removing heavy metals and dyes from aqueous solution using date pits solid adsorbent, J. Hazard. Mater., 176 (2010) 510–520.

[18] S.A. Ahmed, Batch and fixed-bed column techniques for removal of Cu(II) and Fe(III) using carbohydrate natural polymer modified complexing agents, Carbohydr. Polym., 83 (2011) 1470–1478.

[19] X. Li, Y. Tang, X. Cao, D. Lu, F. Luo, W. Shao, Preparation and evaluation of orange peel cellulose adsorbents for effective removal of cadmium, zinc, cobalt and nickel, Colloids Surf., A, 317 (2008) 512–521.

[20] B. Singha, S. Kumar Das, Adsorptive removal of Cu(II) from aqueous solution and industrial effluent using natural/agricultural wastes, Colloids Surf., B, 107 (2013) 97–106.

[21] Guidelines for Drinking-Water Quality, 2nd ed., Vol. 2, Health Criteria and Other Supporting Information, World Health Organization, Geneva, 1996.

[22] WHO, Guidelines for Drinking Water Quality, Recommendations, 2nd ed., Vol. 1, World Health Organization, Geneva, 1993, pp. 39–57, 174.

[23] W. Sloof, R. Cleven, J. Janus, P. van der Poel, Integrated Criteria Document – Chromium, National Institute of Public Health and Environmental Protection, The Netherlands, Report No. 710401002, 1990, 151 p.

[24] J.W. Patterson, Industrial Wastewater Treatment Technology, 2nd ed., Butterworth Publishers, Stoneham, MA, USA, 1985.

[25] US EPA, IRIS, Toxicological Review of Hexavalent Chromium, US Environmental Protection Agency, Washington, D.C., USA, EPA/635/R-10/004A, 2010.

[26] US EPA, IRIS, Toxicological Review of Trivalent Chromium, US Environmental Protection Agency, Washington, D.C., USA, CAS No. (16065-83-1), 1998.

[27] J. Mohammad, M.R. Chandra, S.D. Krishna, Embryotoxicity of orally administered chromium in mice: exposure during the period of organogenesis, Toxicol. Lett., 84 (1996) 143–148.

[28] International Agency for Research on Cancer (IARC), IARC Monographs on the Evaluation of Carcinogenic Risks to Humans, Chromium, Nickel and Welding, Vol. 49, 1990.

[29] J.A. Janus, E.I. Krajnc, Integrated Criteria Document Chromium: Effects, Appendix, Bilthoven, Netherlands, National Institute of Public Health and Environmental Protection, 1990.

[30] N.A. Ibrahim, W.M.W. Yunus, F.A. Abu-Ilaiwi, M.Z. Ab Rahman, M. Bin Ahmad, K.M. Dahlan, Graft copolymerization of methyl methacrylate onto oil palm empty fruit bunch fiber using H_2O_2/Fe^{2+} as an initiator, J. Appl. Polym. Sci., 89 (2003) 2233–2238.

[31] S.S. Tripathy, S. Jena, S.B. Misra, N.P. Padhi, B.C. Singh, A study on graft copolymerization of methyl methacrylate onto jute fiber, J. Appl. Polym. Sci., 30 (1985) 1399–1406.

[32] M.I.H. Mondal, F.I. Farouqui, M. Abdus Salam, Graft copolymerization of acrylate monomers onto sulfonated jute–cotton blended fabric, J. Appl. Polym. Sci., 100 (2006) 4393–4398.

[33] P. Suwanmala, K. Hemvichian, H. Hoshina, W. Srinuttrakul, N. Seko, Preparation of metal adsorbent from poly(methyl acrylate)-grafted-cassava starch via gamma irradiation, Radiat. Phys. Chem., 81 (2012) 982–985.

[34] L. Rahman, S. Silong, W. Md Zin, M.Z. Ab Rahman, M. Ahmad, J. Haron, Graft copolymerization of methyl acrylate onto sago starch using ceric ammonium nitrate as an initiator, J. Appl. Polym. Sci., 76 (2000) 516–523.

[35] A.J. Domb, E.G Cravalho, R. Langer, The synthesis of poly(hydroxamic acid) from poly(acrylamide), J. Polym. Sci., Part A: Polym. Chem., 26 (1988) 2623–2630.

[36] A. Hussain, A. Farooq, M.I. Bassyouni, H.H. Sait, M. Abo El-Wafa, S. Waheedul Hasan, F. Nasir Ani, Pyrolysis of Saudi Arabian date palm waste: a viable option for converting waste into wealth, Life Sci. J., 11 (2014) 667–671.

[37] J. Scheirs, G. Camino, W. Tumiatti, Overview of water evolution during the thermal degradation of cellulose, Eur. Polym. J., 37 (2001) 933–942.

[38] A. Sharma, K.G. Bhattacharyya, Adsorption of chromium (VI) on *Azadirachta indica* (Neem) leaf powder, Adsorption, 10 (2004) 327–338.

[39] V.K. Gupta, I. Ali, T.A. Saleh, M.N. Siddiqui, S. Agarwal, Chromium removal from water by activated carbon developed from waste rubber tires, Environ. Sci. Pollut. Res., 20 (2013) 1261–1268.

[40] Z. AlOthman, M. Naushad, A. Rahmat, Kinetic equilibrium isotherm and thermodynamic studies of Cr(VI) adsorption onto low-cost adsorbent developed from peanut shell activated with phosphoric acid, Environ. Sci. Pollut. Res., 20 (2013) 3351–3365.

[41] D. Hui, Y. Le, T. Guanghui, D. Jiulei, Preparation and characterization of activated carbon from cotton stalk by microwave assisted chemical activation—application in methylene blue adsorption from aqueous solution, J. Hazard. Mater., 166 (2009) 1514–1521.

[42] W.J. Weber, R.K. Chakravarthi, Studies on adsorption of basic dyes on activated carbon, J. Am. Inst. Chem. Eng., 22 (1974) 228–238.

[43] P.K. Malik, Dye removal from wastewater using activated carbon developed from sawdust: adsorption equilibrium and kinetics, J. Hazard. Mater., 113 (2004) 81–88.